Double charm decays of B_c meson in the perturbative QCD approach

Zhou Rui,[1,2] Zhitian Zou,[1] and Cai-Dian Lü[1,*]

[1]*Institute of High Energy Physics and Theoretical Physics Center for Science Facilities, Chinese Academy of Sciences, Beijing 100049, People's Republic of China*

[2]*School of Science, Hebei United University, Tangshan, Hebei 063009, People's Republic of China*

(Received 18 March 2012; revised manuscript received 27 July 2012; published 10 October 2012)

We study the double charm decays of B_c meson, by employing the perturbative QCD approach based on k_T factorization. In this approach, we include the nonfactorizable emission diagrams and W annihilation diagrams, which are neglected in the previous naive factorization approach. The former are important in the color-suppressed modes, while the latter are important in most B_c decay channels owing to the large Cabibbo-Kobayashi-Maskawa matrix elements. We make a comparison with those previous naive factorization results for the branching ratios and also give out the theoretical errors that were previously missed. We predict the transverse polarization fractions of $B_c \to D^{*+}_{(s)}\bar{D}^{*0}$, $D^{*+}_{(s)}D^{*0}$ decays for the first time. A large transverse polarization contribution that can reach 50%–60% is predicted in some of the B_c meson decays.

DOI: 10.1103/PhysRevD.86.074019 PACS numbers: 13.25.Hw, 12.38.Bx, 14.40.Nd

I. INTRODUCTION

Since the B_c meson is the lowest bound state of two different heavy quarks with open flavor, it is stable against strong and electromagnetic annihilation processes. The B_c meson therefore decays weakly. Furthermore, the B_c meson has a sufficiently large mass; thus each of the two heavy quarks can decay individually. It has rich decay channels and provides a very good place to study nonleptonic weak decays of heavy mesons to test the standard model and to search for any new physics signals [1]. The current running LHC collider will produce many more B_c mesons than ever before to make this study a bright future.

Within the standard model, for the double charm decays of $B_{u,d,s}$ mesons, there are penguin operator contributions as well as tree operator contributions. Thus the direct *CP* asymmetry may be present. However, the double charm decays of the B_c meson are pure tree decay modes, which are particularly well suited to extract the Cabibbo-Kobayashi-Maskawa (CKM) angles owing to the absented interference from penguin contributions. As was pointed out in Ref. [2] and further elaborated in Refs. [3–6], the decays $B_c \to D_s^+ D^0$, $D_s^+ \bar{D}^0$ are the gold-plated modes for the extraction of CKM angle γ though amplitude relations because their decay widths are expected to be at the same order of magnitude. But this needs to be examined by faithful calculations.

Although many investigations on the decays of B_c to double-charm states have been carried out [4,5,7–12] in the literature, there are uncontrolled large theoretical errors with quite different numerical results. In fact, all of these old calculations are based on a naive factorization hypothesis, with various form factor inputs. Most of them did not give any theoretical error estimates because of the nonreliability of these models. Recently, the theory of nonleptonic B decays has been improved quite significantly. Factorization has been proved in many of these decays, thus allowing us to give reliable calculations of the hadronic **B** decays. It is also shown that the nonfactorizable contributions and annihilation-type contributions, which are neglected in the naive factorization approach, are very important in these decays [13].

The perturbative QCD approach (pQCD) [14] is one of the recently developed theoretical tools based on QCD to deal with the nonleptonic B decays. Utilizing the k_T factorization instead of collinear factorization, this approach is free of end-point singularity. Thus the Feynman diagrams, including factorizable, nonfactorizable, and annihilation type, are all calculable. Phenomenologically, the pQCD approach successfully predicts the charmless two-body B decays [15,16]. For the decays with a single heavy D meson in the final states [the momentum of the D meson is $\frac{1}{2}m_B(1-r^2)$, with $r = m_D/m_B$], it also proved factorization in the soft-collinear effective theory [17]. Phenomenologically the pQCD approach is also demonstrated to be applicable in the leading order of the m_D/m_B expansion [18,19] for this kind of decays. For the double charm decays of the B_c meson, the momentum of the final state D meson is $\frac{1}{2}m_{B_c}(1-2r^2)$, which is only slightly smaller than that of the decays with a single D meson final state. The proof of factorization here is thus trivial. The pQCD approach is applicable to this kind of decays. In fact, the double charm decays of $B_{u,d,s}$ meson have been studied in the pQCD approach successfully [20,21], with the best agreement with experiments. In this paper, we will extend our study to these B_c decays in the pQCD approach, in order to give predictions on branching ratios and polarization fractions for the experiments to test. Since this

*lucd@ihep.ac.cn

study is based on QCD and perturbative expansion, the theoretical error will be more controllable than any of the model calculations.

Our paper is organized as follows: We review the pQCD factorization approach and then perform the perturbative calculations for these considered decay channels in Sec. II. The numerical results and discussions on the observables are given in Sec. III. The final section is devoted to our conclusions. Some details of related functions and the decay amplitudes are given in the Appendix.

II. FRAMEWORK

For the double charm decays of B_c, only the tree operators of the standard effective weak Hamiltonian contribute. We can divide them into two groups: CKM favored decays with both emission and annihilation contributions and pure emission-type decays, which are CKM suppressed. For the former modes, the Hamiltonian is given by

$$\begin{aligned}\mathcal{H}_{\rm eff} &= \frac{G_F}{\sqrt{2}} V_{cb}^* V_{uq}[C_1(\mu)O_1(\mu) + C_2(\mu)O_2(\mu)],\\ O_1 &= \bar{b}_\alpha \gamma^\mu (1-\gamma_5) c_\beta \otimes \bar{u}_\beta \gamma_\mu (1-\gamma_5) q_\alpha,\\ O_2 &= \bar{b}_\alpha \gamma^\mu (1-\gamma_5) c_\alpha \otimes \bar{u}_\beta \gamma_\mu (1-\gamma_5) q_\beta,\end{aligned} \tag{1}$$

while the effective Hamiltonian of the latter modes reads

$$\begin{aligned}\mathcal{H}_{\rm eff} &= \frac{G_F}{\sqrt{2}} V_{ub}^* V_{cq}[C_1(\mu)O_1'(\mu) + C_2(\mu)O_2'(\mu)],\\ O_1' &= \bar{b}_\alpha \gamma^\mu (1-\gamma_5) u_\beta \otimes \bar{c}_\beta \gamma_\mu (1-\gamma_5) q_\alpha,\\ O_2' &= \bar{b}_\alpha \gamma^\mu (1-\gamma_5) u_\alpha \otimes \bar{c}_\beta \gamma_\mu (1-\gamma_5) q_\beta,\end{aligned} \tag{2}$$

where $V(q = d, s)$ are the corresponding CKM matrix elements; α, β are the color indices; $C_{1,2}$ are Wilson coefficients at renormalization scale μ; and $O_{1,2}$ and $O'_{1,2}$ are the effective four-quark operators.

The factorization theorem allows us to factorize the decay amplitude into the convolution of the hard subamplitude, the Wilson coefficient, and the meson wave functions, all of which are well-defined and gauge invariant. It is expressed as

$$\begin{aligned}&C(t) \otimes H(x,t) \otimes \Phi(x)\\ &\otimes \exp\left[-s(P,b) - 2\int_{1/b}^{t} \frac{d\mu}{\mu}\gamma_q(\alpha_s(\mu))\right],\end{aligned} \tag{3}$$

where $C(t)$ are the corresponding Wilson coefficients of effective operators defined in Eqs. (1) and (2). Since the transverse momentum of the quark is kept in the pQCD approach, the large double logarithm $\ln^2(Pb)$ (with P denoting the longitudinal momentum and b the conjugate variable of the transverse momentum) spoils the perturbative expansion. A resummation is thus needed to give a Sudakov factor $\exp[-s(P,b)]$ [22]. The term after Sudakov is from the renormalization group running with $\gamma_q = -\alpha_s/\pi$, the quark anomalous dimension in axial gauge, and t the factorization scale. All nonperturbative components are organized in the form of hadron wave functions $\Phi(x)$ (with x the longitudinal momentum fraction of valence quark inside the meson), which can be extracted from experimental data or other nonperturbative methods. Since the universal nonperturbative dynamics has been factored out, one can evaluate all possible Feynman diagrams for the hard subamplitude $H(x,t)$ straightforwardly, which include both traditional factorizable and so-called "nonfactorizable" contributions. Factorizable and nonfactorizable annihilation-type diagrams are also calculable without end-point singularity.

A. Channels with both emission and annihilation contributions

At leading order, there are eight kinds of Feynman diagrams contributing to this type of CKM favored decays according to Eq. (1). Here, we take the decay $B_c \to D^+ \bar{D}^0$ as an example, whose Feynman diagrams are shown in Fig. 1. The first line shows the emission-type diagrams, with the first two contributing to the usual form factor; the last two are so-called "nonfactorizable" diagrams. In fact, the first two diagrams are the only contributions calculated in the naive factorization approach. The second line shows the annihilation-type diagrams, with the first two factorizable; the last two are nonfactorizable. The decay amplitude of factorizable diagrams in Figs. 1(a) and 1(b) is

$$\begin{aligned}\mathcal{F}_e = &-2\sqrt{\frac{2}{3}} C_F f_B f_3 \pi M_B^4 \int_0^1 dx_2 \int_0^\infty b_1 b_2 db_1 db_2 \phi_2(x_2)\\ &\times \exp\left(-\frac{b_1^2 \omega_B^2}{2}\right)\{[-(r_2-2)r_b + 2r_2x_2 - x_2]\\ &\times \alpha_s(t_a) h_e(\alpha_e, \beta_a, b_1, b_2) S_t(x_2) \exp[-S_{ab}(t_a)]\\ &+ 2r_2 \alpha_s(t_b) h_e(\alpha_e, \beta_b, b_2, b_1) S_t(x_1) \exp[-S_{ab}(t_b)]\},\end{aligned} \tag{4}$$

where $r_b = m_b/M_B$, $r_i = m_i/M_B (i = 2, 3)$ where m_2, m_3 are the masses of the recoiling charmed meson and the emitting charmed meson, respectively; $C_F = 4/3$ is a color factor; and f_3 is the decay constant of the charmed meson, which is emitted from the weak vertex. The factorization scales $t_{a,b}$ are chosen as the maximal virtuality of internal particles in the hard amplitude, in order to suppress the higher order corrections [23]. The function h_e and the Sudakov factor $\exp[-S]$ are displayed in Appendix B. D meson distribution amplitudes $\phi(x)$ are given in Appendix C. The factor $S_t(x)$ is the jet function resulting from the threshold resummation, whose definitions can be found in Ref. [24].

The formula for nonfactorizable emission diagrams Figs. 1(c) and 1(d) contain the kinematics variables of all three mesons. Its expression is

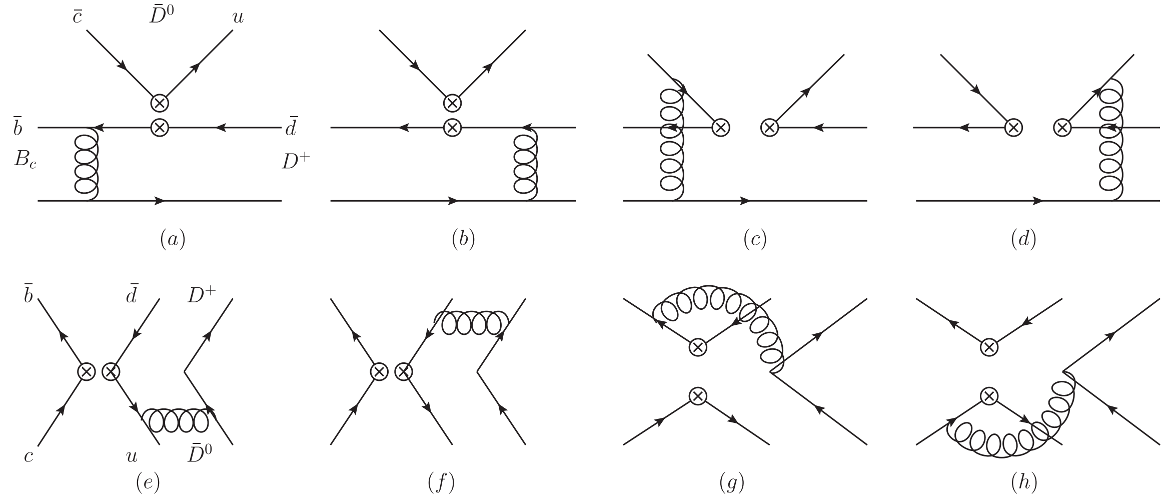

FIG. 1. Feynman diagrams for $B_c \to D^+ \bar{D}^0$ decays.

$$\mathcal{M}_e = -\frac{8}{3} C_F f_B \pi M_B^4 \int_0^1 dx_2 dx_3 \times \int_0^\infty b_2 b_3 db_2 db_3 \phi_2(x_2)\phi_3(x_3) \exp\left(-\frac{b_2^2 \omega_B^2}{2}\right) \times \{[1 - x_1 - x_3 - r_2(1 - x_2)]\alpha_s(t_c) h_e(\beta_c, \alpha_e, b_3, b_2) \times \exp[-S_{cd}(t_c)] - [1 - x_1 - x_2 + x_3 - r_2(1 - x_2)] \times \alpha_s(t_d) h_e(\beta_d, \alpha_e, b_3, b_2) \exp[-S_{cd}(t_d)]\}. \tag{5}$$

Generally, for charmless decays of the B meson, the nonfactorizable contributions of the emission diagrams are small owing to the cancellation between Figs. 1(c) and 1(d). While for double charm decays with the light meson replaced by a charmed meson, since the heavy $\bar{c}$ quark and the light quark are not symmetric, the nonfactorizable emission diagrams ought to give remarkable contributions. This has been shown in the pQCD calculation of $B \to D\pi$ decays for very large branching ratios of color-suppressed modes [25] and proved by the B factory experiments.

The decay amplitude of factorizable annihilation diagrams Figs. 1(e) and 1(f) involve only the two final states charmed meson wave functions, shown as

$$\mathcal{F}_a = -8 C_F f_B \pi M_B^4 \int_0^1 dx_2 dx_3 \times \int_0^\infty b_2 b_3 db_2 db_3 \phi_2(x_2)\phi_3(x_3)\{[1 - x_2] \times \alpha_s(t_e) h_e(\alpha_a, \beta_e, b_2, b_3) \exp[-S_{ef}(t_e)] S_t(x_3) - [1 - x_3]\alpha_s(t_f) h_e(\alpha_a, \beta_f, b_3, b_2) \times \exp[-S_{ef}(t_f)] S_t(x_2)\}. \tag{6}$$

For the nonfactorizable annihilation diagrams Figs. 1(g) and 1(h), the decay amplitude is

$$\mathcal{M}_a = \frac{8}{3} C_F f_B \pi M_B^4 \int_0^1 dx_2 dx_3 \times \int_0^\infty b_1 b_2 db_1 db_2 \phi_2(x_2)\phi_3(x_3) \exp\left(-\frac{b_1^2 \omega_B^2}{2}\right) \times \{[x_1 + x_3 - 1 - r_c]\alpha_s(t_g) h_e(\beta_g, \alpha_a, b_1, b_2) \times \exp[-S_{gh}(t_g)] - [r_b - x_2]\alpha_s(t_h) h_e(\beta_h, \alpha_a, b_1, b_2) \times \exp[-S_{gh}(t_h)]\}, \tag{7}$$

where $r_c = m_c/M_B$, with m_c the mass of the c quark in the B_c meson. Finally, the total decay amplitude for $B_c \to D^+ \bar{D}^0$ can be given by

$$\mathcal{A}(B_c \to D^+ \bar{D}^0) = V_{cb}^* V_{ud}[a_2 \mathcal{F}_e + C_2 \mathcal{M}_e + a_1 \mathcal{F}_a + C_1 \mathcal{M}_a], \tag{8}$$

with the combinations of Wilson coefficients $a_1 = C_2 + C_1/3$ and $a_2 = C_1 + C_2/3$, characterizing the color-favored contribution and the color-suppressed contribution in the naive factorization, respectively. The total decay amplitudes of $B_c \to D_s^+ \bar{D}^0$, $B_c \to D^+ \bar{D}^{*0}$, and $B_c \to D_s^+ \bar{D}^{*0}$ can be obtained from Eq. (8) with the following replacement:

$$\begin{aligned} &\mathcal{A}(B_c \to D_s^+ \bar{D}^0) \\ &\quad = V_{cb}^* V_{us}[a_2 \mathcal{F}_e + C_2 \mathcal{M}_e + a_1 \mathcal{F}_a + C_1 \mathcal{M}_a]|_{D^+ \to D_s^+}, \\ &\mathcal{A}(B_c \to D^+ \bar{D}^{*0}) \\ &\quad = V_{cb}^* V_{ud}[a_2 \mathcal{F}_e + C_2 \mathcal{M}_e + a_1 \mathcal{F}_a + C_1 \mathcal{M}_a]|_{\bar{D}^0 \to \bar{D}^{*0}}, \\ &\mathcal{A}(B_c \to D_s^+ \bar{D}^{*0}) \\ &\quad = V_{cb}^* V_{us}[a_2 \mathcal{F}_e + C_2 \mathcal{M}_e + a_1 \mathcal{F}_a + C_1 \mathcal{M}_a]|_{D^+ \to D_s^+, \bar{D}^0 \to \bar{D}^{*0}}. \end{aligned} \tag{9}$$

Comparing our Eqs. (8) and (9) with the formulas of the previous naive factorization approach [4,5,7–10], it is easy to see that only the first term appearing in Eqs. (8) and (9)

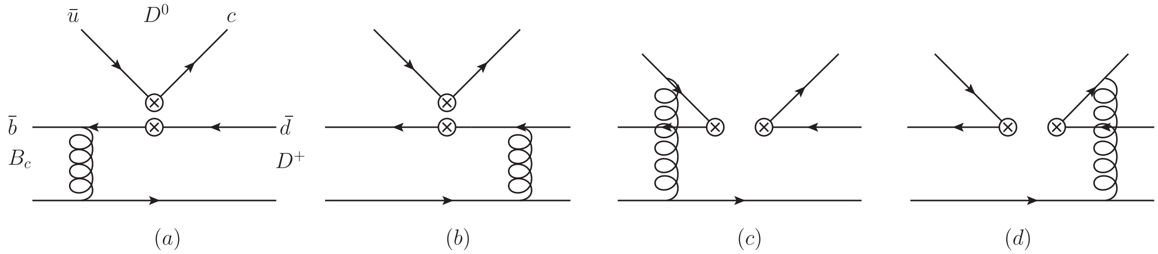

FIG. 2. Color-suppressed emission diagrams contributing to the $B_c \to D^+ D^0$ decays.

are calculated in the previous naive factorization approach. The second, third, and fourth terms in these equations are the corresponding nonfactorizable emission-type, factorizable annihilation-type, and nonfactorizable annihilation-type contributions, respectively, which are all new calculations.

In $B_c \to D_{(s)}^{*+}\bar{D}^{*0}$ decays, the two vector mesons in the final states have the same helicity owing to angular momentum conservation; therefore only three different polarization states, one longitudinal and two transverse for both vector mesons, are possible. The decay amplitude can be decomposed as

$$\mathcal{A} = \mathcal{A}^L + \mathcal{A}^N \epsilon_2^T \cdot \epsilon_3^T + i\mathcal{A}^T \epsilon_{\alpha\beta\rho\sigma} n^\alpha v^\beta \epsilon_2^{T\rho} \epsilon_3^{T\sigma}, \qquad (10)$$

where ϵ_2^T, ϵ_3^T are the transverse polarization vectors for the two vector charmed mesons, respectively. $\mathcal{A}^L$ corresponds to the contributions of longitudinal polarization; $\mathcal{A}^N$ and $\mathcal{A}^T$ correspond to the contributions of normal and transverse polarization, respectively. And the total amplitudes $\mathcal{A}^{L,N,T}$ have the same structures as Eqs. (8) and (9). The factorization formulas for the longitudinal, normal, and transverse polarizations are listed in Appendix A.

For $B_c \to D_{(s)}^{*+}\bar{D}^0$ decays, only the longitudinal polarization of the $D_{(s)}^{*+}$ meson will contribute, owing to the angular momentum conservation. We can obtain their decay amplitudes from the longitudinal polarization amplitudes for the $B_c \to D_{(s)}^{*+}\bar{D}^{*0}$ decays with the replacement $\bar{D}^{*0} \to \bar{D}^0$.

B. Channels with pure emission-type decays

There are also eight kinds of Feynman diagrams contributing to $B_c \to D_{(s)}^{(*)+} D^{(*)0}$ decays according to Eq. (2), but all are emission type. Taking the decay $B_c \to D^+ D^0$ as an example, Fig. 2 shows the color-suppressed emission diagrams while Fig. 3 shows the color-favored emission diagrams. We mark the subscripts 2 and 3 to denote the contributions from Figs. 2 and 3, respectively. The decay amplitude of factorization emission diagrams $\mathcal{F}_{e2}$, coming from Figs. 2(a) and 2(b), is similar to Eq. (4), but with the replacement $\bar{D}^0 \to D^0$. While the decay amplitude of the nonfactorization emission diagram $\mathcal{M}_{e2}$, coming from Figs. 2(c) and 2(d), is different from Eq. (5), the heavy c quark and the light antiquark are not symmetric. The expression of the nonfactorizable emission diagram is

$$\begin{aligned}
\mathcal{M}_{e2} = &-\frac{8}{3} C_F f_B \pi M_B^4 \int_0^1 dx_2 dx_3 \\
&\times \int_0^\infty b_2 b_3 db_2 db_3 \phi_2(x_2)\phi_3(x_3) \exp\left(-\frac{b_2^2\omega_B^2}{2}\right) \\
&\times \{[2 - x_1 - x_2 - x_3 - r_2(1 - x_2)] \\
&\times \alpha_s(t_c) h_e(\beta_c, \alpha_e, b_3, b_2) \exp[-S_{cd}(t_c)] \\
&- [x_3 - x_1 - r_2(1 - x_2)]\alpha_s(t_d) h_e(\beta_d, \alpha_e, b_3, b_2) \\
&\times \exp[-S_{cd}(t_d)]\}. \qquad (11)
\end{aligned}$$

By exchanging the two final states charmed mesons in Fig. 2, one can obtain the corresponding decay amplitudes formulas $\mathcal{F}_{e3}$ and $\mathcal{M}_{e3}$ for Fig. 3. The total decay amplitude of $B_c \to D^+ D^0$ decay can be written as

$$\begin{aligned}
&\mathcal{A}(B_c \to D^+ D^0) \\
&\quad = V_{ub}^* V_{cd}[a_2 \mathcal{F}_{e2} + C_2 \mathcal{M}_{e2} + a_1 \mathcal{F}_{e3} + C_1 \mathcal{M}_{e3}]. \qquad (12)
\end{aligned}$$

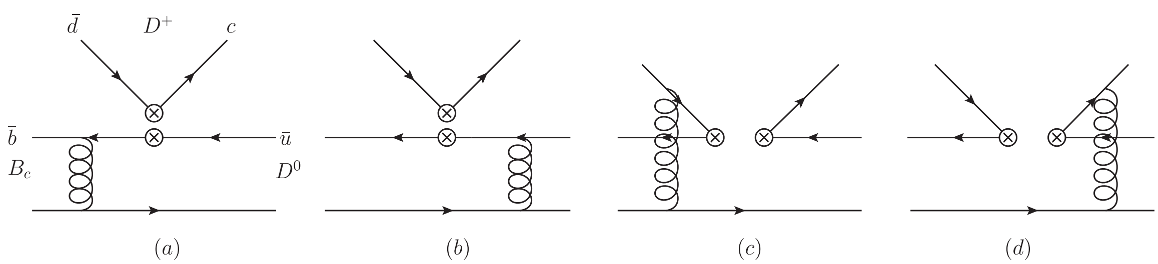

FIG. 3. Color-favored emission diagrams contributing to the $B_c \to D^+ D^0$ decays.

If the final recoiling meson is the vector D^* meson, the decay amplitudes of factorization emission diagrams and nonfactorization emission diagrams are given as

$$\mathcal{F}^*_{e2} = -2\sqrt{\frac{2}{3}}C_F f_B f_3 \pi M_B^4 \int_0^1 dx_2 \int_0^\infty b_1 b_2 db_1 db_2 \phi_2(x_2) \exp\left(-\frac{b_1^2\omega_B^2}{2}\right)\{[-(r_2-2)r_b + 2r_2x_2 - x_2] \times \alpha_s(t_a)h_e(\alpha_e, \beta_a, b_1, b_2)S_t(x_2)\exp[-S_{ab}(t_a)] + r_2^2\alpha_s(t_b)h_e(\alpha_e, \beta_b, b_2, b_1)S_t(x_1)\exp[-S_{ab}(t_b)]\}, \tag{13}$$

$$\mathcal{M}^*_{e2} = -\frac{8}{3}C_F f_B \pi M_B^4 \int_0^1 dx_2 dx_3 \int_0^\infty b_2 b_3 db_2 db_3 \phi_2(x_2)\phi_3(x_3) \exp\left(-\frac{b_2^2\omega_B^2}{2}\right) \times \{[2 - x_1 - x_2 - x_3 - r_2(1-x_2)]\alpha_s(t_c)h_e(\beta_c, \alpha_e, b_3, b_2)\exp[-S_{cd}(t_c)] - [x_3 - x_1 + r_2(1-x_2)]\alpha_s(t_d)h_e(\beta_d, \alpha_e, b_3, b_2)\exp[-S_{cd}(t_d)]\}. \tag{14}$$

The total decay amplitudes for other pure emission-type decays are then

$$\begin{aligned}
\mathcal{A}(B_c \to D_s^+ D^0) &= V^*_{ub}V_{cs}[a_2\mathcal{F}_{e2} + C_2\mathcal{M}_{e2} + a_1\mathcal{F}_{e3} + C_1\mathcal{M}_{e3}],\\
\mathcal{A}(B_c \to D^+ D^{*0}) &= V^*_{ub}V_{cd}[a_2\mathcal{F}_{e2} + C_2\mathcal{M}_{e2} + a_1\mathcal{F}^*_{e3} + C_1\mathcal{M}^*_{e3}],\\
\mathcal{A}(B_c \to D^{*+} D^0) &= V^*_{ub}V_{cd}[a_2\mathcal{F}^*_{e2} + C_2\mathcal{M}^*_{e2} + a_1\mathcal{F}_{e3} + C_1\mathcal{M}_{e3}],\\
\mathcal{A}(B_c \to D_s^+ D^{*0}) &= V^*_{ub}V_{cs}[a_2\mathcal{F}_{e2} + C_2\mathcal{M}_{e2} + a_1\mathcal{F}^*_{e3} + C_1\mathcal{M}^*_{e3}],\\
\mathcal{A}(B_c \to D_s^{*+} D^0) &= V^*_{ub}V_{cs}[a_2\mathcal{F}^*_{e2} + C_2\mathcal{M}^*_{e2} + a_1\mathcal{F}_{e3} + C_1\mathcal{M}_{e3}].
\end{aligned} \tag{15}$$

The $B_c \to D^{*+}_{(s)} D^{*0}$ decays have a similar situation to $B_c \to D^{*+}_{(s)} \bar{D}^{*0}$, their factorization formulas are also listed in Appendix A.

III. NUMERICAL RESULTS

In this section, we summarize the numerical results and analysis in the double charm decays of the B_c meson. Some input parameters needed in the pQCD calculation are listed in Table I.

A. The form factors

The diagrams in Figs. 1(a) and 1(b) or Figs. 3(a) and 3(b) give the contribution for the $B_c \to D^{(*)}_{(s)}$ transition form factor at the $q^2 = 0$ point. Our predictions of the form factors are collected in Table II. The error is from the combined uncertainty in the hadronic parameters: (1) the shape parameters: $\omega_B = 0.60 \pm 0.05$ for the B_c meson wave function, $a_D = (0.5 \pm 0.1)$ GeV for the $D^{(*)}$ meson, and $a_{D_s} = (0.4 \pm 0.1)$ GeV for the $D_s^{(*)}$ meson wave

TABLE I. Parameters we used in numerical calculation [26].

Mass [GeV]	$M_W = 80.399$	$M_{B_c} = 6.277$ $\quad m_b = 4.2$	$m_c = 1.27$
CKM	$\lvert V_{ub}\rvert = (3.47^{+0.16}_{-0.12}) \times 10^{-3}$	$\lvert V_{ud}\rvert = 0.97428^{+0.00015}_{-0.00015}$	$\lvert V_{us}\rvert = 0.2253^{+0.0007}_{-0.0007}$
	$\lvert V_{cs}\rvert = 0.97345^{+0.00015}_{-0.00016}$	$\lvert V_{cd}\rvert = 0.2252^{+0.0007}_{-0.0007}$	$\lvert V_{cb}\rvert = 0.0410^{+0.0011}_{-0.0007}$
Decay constants (MeV)	$f_{B_c} = 489$	$f_D = 206.7 \pm 8.9$	$f_{D_s} = 257.5 \pm 6.1$
Lifetime			$\tau_{B_c} = 0.453 \times 10^{-12}$ s

TABLE II. The form factors for $B_c \to D^{(*)}_{(s)}$ at $q^2 = 0$ evaluated in the pQCD approach. The uncertainties are from the hadronic parameters. For comparison, we also cite the theoretical estimates of other models.

	This work	Kiselev Ref. [4][a]	IKP Ref. [5]	WSL Ref. [27]	DSV Ref. [28]	DW Ref. [29][b]
$F^{B_c\to D}$	$0.14^{+0.01}_{-0.02}$	0.32 [0.29]	0.189	0.16	0.075	0.255
$F^{B_c\to D_s}$	$0.19^{+0.02}_{-0.01}$	0.45 [0.43]	0.194	0.28	0.15	...
$A_0^{B_c\to D^*}$	$0.12^{+0.02}_{-0.01}$	0.35 [0.37]	0.133	0.09	0.081	0.257
$A_0^{B_c\to D_s^*}$	$0.17^{+0.01}_{-0.01}$	0.47 [0.52]	0.142	0.17	0.16	...

[a]The nonbracketed (bracketed) results are evaluated in sum rules (potential model).
[b]We quote the result with $\omega = 0.7$ GeV.

TABLE III. Branching ratios (10^{-6}) of the CKM favored decays with both emission and annihilation contributions, together with results from other models. The errors for these entries correspond to the uncertainties in the input hadronic quantities, from the CKM matrix elements and the scale dependence, respectively.

	Channels	This work	Kiselev Ref. [4]	IKP Ref. [5]	IKS Ref. [7]	LC Ref. [8]	CF Ref. [10]
1	$B_c \to D^+ \bar{D}^0$	32^{+6+1+2}_{-6-1-4}	53	32	33	86	8.4
2	$B_c \to D^+ \bar{D}^{*0}$	34^{+7+2+3}_{-6-1-3}	75	83	38	75	7.5
3	$B_c \to D^{*+} \bar{D}^0$	12^{+3+1+0}_{-3-0-1}	49	17	9	30	84
4	$B_c \to D^{*+} \bar{D}^{*0}$	34^{+9+2+0}_{-8-1-0}	330	84	21	55	140
5	$B_c \to D_s^+ \bar{D}^0$	$2.3^{+0.4+0.1+0.2}_{-0.4-0.1-0.2}$	4.8	1.7	2.1	4.6	0.6
6	$B_c \to D_s^+ \bar{D}^{*0}$	$2.6^{+0.4+0.1+0.1}_{-0.6-0.1-0.2}$	7.1	4.3	2.4	3.9	0.53
7	$B_c \to D_s^{*+} \bar{D}^0$	$0.7^{+0.1+0.0+0.0}_{-0.2-0.0-0.0}$	4.5	0.95	0.65	1.8	5
8	$B_c \to D_s^{*+} \bar{D}^{*0}$	$2.8^{+0.7+0.1+0.1}_{-0.6-0.1-0.0}$	26	4.7	1.6	3.5	8.4

function [20]; (2) the decay constants in the wave functions of charmed mesons, which are given in Table I. Since the uncertainties from decay constants of $D_{(s)}$ and the shape parameters of the wave functions are very small, the relevant uncertainties to the form factors are also very small. We can see that the $SU(3)$ symmetry breaking effects between B_c to $D^{(*)}$ and B_c to $D_s^{(*)}$ form factors are large, as the decay constant of D_s is about one-fifth larger than that of the D meson.

In the literature there are already lots of studies on $B_c \to D_{(s)}^{(*)}$ transition form factors [4,5,27–29], whose results are collected in Table II. Our results are generally close to the covariant light-front quark model results of Ref. [27] and the constituent quark model results of Ref. [5]. However, other results collected in Table II, especially for the QCD sum rules [4] and the Bauer, Stech, and Wirbel model [28], deviate a lot numerically. The predictions of QCD sum rules [4] are larger than those in other works [5,27–29]. The reason is that they have taken into account the α_s/v corrections and the form factors are enhanced by 3 times owing to the Coulomb renormalization of the quark-meson vertex for the heavy quarkonium B_c. The results of the Bauer, Stech, and Wirbel model [28] are quite small owing to a smaller overlap of the initial and final states wave functions. Although, the included flavor dependence of the average transverse quark momentum in the mesons can enhance the form factors for $B_c \to D^*_{(s)}$ transitions, their predictions are still smaller than other models. The large differences in different models can be discriminated by the future LHC experiments.

B. Branching ratios

With the decays amplitudes $\mathcal{A}$ obtained in Sec. II, the branching ratio $\mathcal{BR}$ reads as

$$\mathcal{BR} = \frac{G_F \tau_{B_c}}{32\pi M_B}\sqrt{(1-(r_2+r_3)^2)(1-(r_2-r_3)^2)}|\mathcal{A}|^2. \tag{16}$$

As stated in Sec. II, the contributions from the penguin operators are absent, since the penguins add an even number of charmed quarks, while there is already one from the initial state. There should be no CP violation in these processes. We tabulate the branching ratios of the considered decays in Tables III and IV. The processes (1)–(4) in

TABLE IV. Branching ratios (10^{-7}) of the CKM suppressed decays with pure emission contributions, together with results from other models. The errors for these entries correspond to the uncertainties in the input hadronic quantities, from the CKM matrix elements and the scale dependence, respectively.

	Channels	This work	Kiselev Ref. [4]	IKP Ref. [5]	IKS Ref. [7]
1	$B_c \to D^+ D^0$	$1.0^{+0.2+0.1+0.0}_{-0.1-0.0-0.0}$	3.2	1.1	3.1
2	$B_c \to D^+ D^{*0}$	$0.7^{+0.1+0.1+0.0}_{-0.2-0.0-0.0}$	2.8	0.25	0.52
3	$B_c \to D^{*+} D^0$	$0.9^{+0.1+0.1+0.0}_{-0.2-0.0-0.0}$	4.0	3.8	4.4
4	$B_c \to D^{*+} D^{*0}$	$0.8^{+0.2+0.1+0.2}_{-0.1-0.0-0.0}$	15.9	2.8	2.0
5	$B_c \to D_s^+ D^0$	30^{+5+3+1}_{-4-2-1}	66	25	74
6	$B_c \to D_s^+ D^{*0}$	19^{+3+2+0}_{-3-1-1}	63	6	13
7	$B_c \to D_s^{*+} D^0$	25^{+4+2+0}_{-3-2-1}	85	69	93
8	$B_c \to D_s^{*+} D^{*0}$	24^{+3+2+1}_{-3-2-1}	404	54	45

Table III have a comparatively large branching ratio (10^{-5}) with the CKM factor $V_{cb}^* V_{ud} \sim \lambda^2$, while the branching ratios of other processes are relatively small owing to the CKM factor suppression. Especially for the processes (1)–(4) in Table IV, these channels are suppressed by CKM elements V_{ub}/V_{cb} and V_{cd}/V_{ud}. Thus their branching ratios are 3 orders of magnitude smaller.

For comparison, we also cite other theoretical results [4,5,7,8,10] for the double charm decays of the B_c meson in Tables III and IV. In general, the results of the various model calculations are of the same order of magnitude for most channels. However, the difference between different model calculations is quite large. This is expected from the large difference of input parameters, especially the large difference of form factors shown in Table II. As stated in the Introduction, all the calculations of these B_c to two D meson decays in the literature use the same naive factorization approach. Their difference relies only on the input form factors and decay constants. Therefore the comparison of results with any of them is straightforward. Larger branching ratios always come with the larger form factors. As stated in the previous subsection, our results of form factors are comparable with the relativistic constituent quark model [5,7], and thus our branching ratios in Table III are also comparable with theirs except for the processes $B_c \to D^{*+} \bar{D}^{*0}$ and $B_c \to D_s^{*+} \bar{D}^{*0}$. Because of the sizable contributions of transverse polarization amplitudes, our branching ratios are larger than those in the relativistic constituent quark model, whose transverse contribution is negligible.

Since all the previous calculations in the literature are model calculations, it is difficult for them to give the theoretical error estimations. In our pQCD approach, the factorization holds at the leading order expansion of m_D/m_B. At this order, we can do the systematical calculation, so as to determine the error estimations in the tables. The first error in these entries is estimated from the hadronic parameters: (1) the shape parameters: $\omega_B = 0.60 \pm 0.05$ for the B_c meson, $a_D = (0.5 \pm 0.1)$ GeV for the $D^{(*)}$ meson, and $a_{D_s} = (0.4 \pm 0.1)$ GeV for the $D_s^{(*)}$ meson [20]; (2) the decay constants in the wave functions of charmed mesons, which are given in Table I. The second error is from the uncertainty in the CKM matrix elements, which are also given in Table I. The third error arises from the hard scale t varying from $0.75t$ to $1.25t$, which characterizes the size of next-to-leading order QCD contributions. The small errors of this type indicate that our perturbative expansion indeed holds. It is easy to see that the most important uncertainty in our approach comes from the hadronic parameters. The total theoretical error is in general about 10% to 30% in size.

The eight CKM favored channels (proportional to $|V_{cb}|$) in Table III receive contributions from both emission diagrams and annihilation diagrams. From Fig. 1, one can find that the contributions from the factorizable emission diagrams are color suppressed. The naive factorization approach cannot give reliable predictions because of large nonfactorizable contributions [30]. As was pointed out in Sec. II, the nonfactorizable emission diagrams give large contributions in the pQCD approach because of the asymmetry of the two quarks in charmed mesons. Thus, the branching ratios of these decays are dominated by the nonfactorizable emission diagrams.

The eight CKM suppressed channels (proportional to $|V_{ub}|$) in Table IV can occur only via emission-type diagrams. There are two types of emission diagrams in these decays, one is color suppressed and one is color favored. It is expected that the color-favored factorizable amplitude $\mathcal{F}_{e3}$ dominates in Eq. (15). However, the nonfactorizable contribution $\mathcal{M}_{e2}$, proportional to the large C_2, is enhanced by the Wilson coefficient. Numerically it is indeed comparable to the color-favored factorizable amplitude. This large nonfactorizable contribution has already been shown in the similar $B \to D\pi$ decays theoretically and experimentally [25]. In all of these channels the nonfactorizable contributions play a very important role; therefore the branching ratios predicted in Tables III and IV are not like the previous naive factorization approach calculations [4,5,7,8,10]. They are not simply proportional to the corresponding form factors any more, but with a very complicated manner, since we have also additional annihilation-type contributions.

From Tables III and IV, one can see that as was expected the magnitudes of the branching ratios of the decays $B_c \to D_s^+ \bar{D}^0$ and $B_c \to D_s^+ D^0$ are very close to each other. In our numerical results, the ratio of the two decay widths is estimated as $\frac{\Gamma(B_c \to D_s^+ D^0)}{\Gamma(B_c \to D_s^+ \bar{D}^0)} \approx 1.3$. They are very suitable for extracting the CKM angle γ through the amplitude relations. Hopefully they will be measured in the experiments soon. However, the decays $B_c \to D^+ \bar{D}^0$, $D^+ D^0$ are problematic from the methodic point of view for $\mathcal{BR}(B_c \to D^+ D^0) \ll \mathcal{BR}(B_c \to D^+ \bar{D}^0)$. The corresponding ratio in $B_c \to D^+ D^0$, $D^+ \bar{D}^0$ decays is $\frac{\Gamma(B_c \to D^+ D^0)}{\Gamma(B_c \to D^+ \bar{D}^0)} \sim 10^{-3}$, which confirm the latter decay modes are not useful to determine the angle γ experimentally.

For the B_c decays to two vector mesons, the decay amplitudes $\mathcal{A}$ are defined in the helicity basis

$$\mathcal{A} = \sum_{i=0,+,-} |\mathcal{A}_i|^2, \tag{17}$$

where the helicity amplitudes $\mathcal{A}_i$ have the following relationships with $\mathcal{A}^{L,N,T}$:

$$\mathcal{A}_0 = \mathcal{A}^L, \qquad \mathcal{A}_\pm = \mathcal{A}^N \pm \mathcal{A}^T. \tag{18}$$

We also calculate the transverse polarization fractions $\mathcal{R}_T$ of the $B_c \to D_{(s)}^* D^*$ decays, with the definition given by

$$\mathcal{R}_T = \frac{|\mathcal{A}_+|^2 + |\mathcal{A}_-|^2}{|\mathcal{A}_0|^2 + |\mathcal{A}_+|^2 + |\mathcal{A}_-|^2}. \tag{19}$$

TABLE V. The transverse polarizations fractions (%) for $B_c \to VV$. The errors correspond to the uncertainties in the hadronic parameters and the scale dependence, respectively.

	$B_c \to D^{*+}\bar{D}^{*0}$	$B_c \to D_s^{*+}\bar{D}^{*0}$	$B_c \to D^{*+}D^{*0}$	$B_c \to D_s^{*+}D^{*0}$
$\mathcal{R}_T$	58^{+3+1}_{-3-0}	68^{+2+1}_{-2-1}	4^{+1+1}_{-1-1}	6^{+1+2}_{-0-1}

These should be the first theoretical predictions in the literature, which are absent in all the naive factorization calculations. According to the power counting rules in the factorization assumption, the longitudinal polarization should be dominant owing to the quark helicity analysis. Our predictions for the transverse polarization fractions of the decays $B_c \to D_{(s)}^{*+}D^{*0}$, which are given in Table V, are indeed small, since the two transverse amplitudes are down by a power of r_2 or r_3 comparing with the longitudinal amplitudes. However, for $B_c \to D_{(s)}^{*+}\bar{D}^{*0}$ decays, the most important contributions for these two decay channels are from the nonfactorizable tree diagrams in Figs. 1(c) and 1(d). With an additional gluon, the transverse polarization in the nonfactorizable diagrams does not encounter helicity flip suppression. The transverse polarization is at the same order as longitudinal polarization. Therefore, we can expect the transverse polarizations to take a larger ratio in the branching ratios, which can reach ~60%. The fact that the nonfactorizable contribution can give a large transverse polarization contribution is also observed in the $B^0 \to \rho^0\rho^0$, $\omega\omega$ decays [31] and in the $B_c \to D_s^{*+}\omega$ decay [32].

IV. CONCLUSION

All the previous calculations in the literature for the B_c meson decays to two charmed mesons are based on the very simple naive factorization approach. The branching ratios predicted in this kind of model calculation depend heavily on the input form factors. Since all of these modes contain dominant or large contributions from color-suppressed diagrams, the predicted branching ratios are also not stable owing to the large unknown nonfactorizable contributions. In this paper, we have performed a systematic analysis of the double charm decays of the B_c meson in the pQCD approach based on the k_T factorization theorem, which is free of end-point singularities. All topologies of decay amplitudes are calculable in the same framework, including the nonfactorizable one and the annihilation type. It is found that the nonfactorizable emission diagrams give a remarkable contribution. There is no CP violation for all these decays within the standard model, since there are only tree operator contributions. The predicted branching ratios range from very small numbers of $\mathcal{O}(10^{-8})$ up to the largest branching fraction of $\mathcal{O}(10^{-5})$. Since all of the previous naive factorization calculations did not give the theoretical uncertainty in the numerical results, it is not easy to compare our results with theirs. The theoretical uncertainty study in the pQCD approach shows that our numerical results are reliable, which may be tested in the upcoming experimental measurements. We predict the transverse polarization fractions of the B_c decays with two vector D^* mesons in the final states for the first time. Because of the cancellation of some hadronic parameters in the ratio, the polarization fractions are predicted with less theoretical uncertainty. The transverse polarization fractions are large in some channels, which mainly come from the nonfactorizable emission diagrams.

ACKNOWLEDGMENTS

We thank Hsiang-nan Li and Fusheng Yu for helpful discussions. This work is partially supported by National Natural Science Foundation of China under Grant No. 11075168, Natural Science Foundation of Zhejiang Province of China, Grant No. Y606252, and Scientific Research Fund of Zhejiang Provincial Education Department of China, Grant No. 20051357.

APPENDIX A: FACTORIZATION FORMULAS FOR $B_c \to VV$

In the B_c decays to two vector meson final states, we use the superscripts L, N, and T to denote the contributions from longitudinal polarization, normal polarization, and transverse polarization, respectively. For the CKM favored $B_c \to D_{(s)}^{*+}\bar{D}^{*0}$ decays, the decay amplitudes for different polarizations are

$$\mathcal{F}_e^L = -2\sqrt{\frac{2}{3}}C_F f_B f_3 \pi M_B^4 \int_0^1 dx_2 \int_0^\infty b_1 b_2 db_1 db_2 \phi_2(x_2) \exp\left(-\frac{b_1^2\omega_B^2}{2}\right)\{[-(r_2-2)r_b + 2r_2x_2 - x_2]\alpha_s(t_a) \times h_e(\alpha_e, \beta_a, b_1, b_2)S_t(x_2)\exp[-S_{ab}(t_a)] + r_2^2\alpha_s(t_b)h_e(\alpha_e, \beta_b, b_2, b_1)S_t(x_1)\exp[-S_{ab}(t_b)]\}, \tag{A1}$$

$$\mathcal{M}_e^L = -\frac{8}{3}C_F f_B \pi M_B^4 \int_0^1 dx_2 dx_3 \int_0^\infty b_2 b_3 db_2 db_3 \phi_2(x_2)\phi_3(x_3)\exp\left(-\frac{b_2^2\omega_B^2}{2}\right)\{[1-x_1-x_3 + r_2(1-x_2)]\alpha_s(t_c)h_e(\beta_c, \alpha_e, b_3, b_2)\exp[-S_{cd}(t_c)] - [1-x_1-x_2+x_3-r_2(1-x_2)] \times \alpha_s(t_d)h_e(\beta_d, \alpha_e, b_3, b_2)\exp[-S_{cd}(t_d)]\}, \tag{A2}$$

$$\mathcal{F}_a^L = -8C_F f_B \pi M_B^4 \int_0^1 dx_2 dx_3 \int_0^\infty b_2 b_3 db_2 db_3 \phi_2(x_2)\phi_3(x_3)\{[1-x_2]\alpha_s(t_e)h_e(\alpha_a, \beta_e, b_2, b_3) \times \exp[-S_{ef}(t_e)]S_t(x_3) - [1-x_3]\alpha_s(t_f)h_e(\alpha_a, \beta_f, b_3, b_2)\exp[-S_{ef}(t_f)]S_t(x_2)\}, \tag{A3}$$

$$\mathcal{M}_a^L = \frac{8}{3}C_F f_B \pi M_B^4 \int_0^1 dx_2 dx_3 \int_0^\infty b_1 b_2 db_1 db_2 \phi_2(x_2)\phi_3(x_3)\exp\left(-\frac{b_1^2\omega_B^2}{2}\right)\{[x_1+x_3-1-r_c]\alpha_s(t_g)h_e(\beta_g, \alpha_a, b_1, b_2) \times \exp[-S_{gh}(t_g)] - [r_b - x_2]\alpha_s(t_h)h_e(\beta_h, \alpha_a, b_1, b_2)\exp[-S_{gh}(t_h)]\}, \tag{A4}$$

$$\mathcal{F}_e^N = -2\sqrt{\frac{2}{3}}C_F f_B f_3 r_3 \pi M_B^4 \int_0^1 dx_2 \int_0^\infty b_1 b_2 db_1 db_2 \phi_2(x_2)\exp\left(-\frac{b_1^2\omega_B^2}{2}\right)\{[2-r_b+r_2(4r_b-x_2-1)] \times \alpha_s(t_a)h_e(\alpha_e, \beta_a, b_1, b_2)S_t(x_2)\exp[-S_{ab}(t_a)] - r_2\alpha_s(t_b)h_e(\alpha_e, \beta_b, b_2, b_1)S_t(x_1)\exp[-S_{ab}(t_b)]\}, \tag{A5}$$

$$\mathcal{F}_e^T = 2\sqrt{\frac{2}{3}}C_F f_B f_3 r_3 \pi M_B^4 \int_0^1 dx_2 \int_0^\infty b_1 b_2 db_1 db_2 \phi_2(x_2)\exp\left(-\frac{b_1^2\omega_B^2}{2}\right)\{[2-r_b-r_2(1-x_2)] \times \alpha_s(t_a)h_e(\alpha_e, \beta_a, b_1, b_2)S_t(x_2)\exp[-S_{ab}(t_a)] - r_2\alpha_s(t_b)h_e(\alpha_e, \beta_b, b_2, b_1)S_t(x_1)\exp[-S_{ab}(t_b)]\}, \tag{A6}$$

$$\begin{aligned}\mathcal{M}_e^N &= -\mathcal{M}_e^T \\ &= \frac{8}{3}C_F f_B \pi M_B^4 r_3 \int_0^1 dx_2 dx_3 \int_0^\infty b_2 b_3 db_2 db_3 \phi_2(x_2)\phi_3(x_3)\exp\left(-\frac{b_2^2\omega_B^2}{2}\right)\{[x_1+x_3-1]\alpha_s(t_c)h_e(\beta_c, \alpha_e, b_3, b_2) \\ &\times \exp[-S_{cd}(t_c)] - [x_1-x_3]\alpha_s(t_d)h_e(\beta_d, \alpha_e, b_3, b_2)\exp[-S_{cd}(t_d)]\},\end{aligned} \tag{A7}$$

$$\mathcal{F}_a^N = -8C_F f_B \pi M_B^4 r_2 r_3 \int_0^1 dx_2 dx_3 \int_0^\infty b_2 b_3 db_2 db_3 \phi_2(x_2)\phi_3(x_3)\{[2-x_2]\alpha_s(t_e)h_e(\alpha_a, \beta_e, b_2, b_3) \times \exp[-S_{ef}(t_e)]S_t(x_3) - [2-x_3]\alpha_s(t_f)h_e(\alpha_a, \beta_f, b_3, b_2)\exp[-S_{ef}(t_f)]S_t(x_2)\}, \tag{A8}$$

$$\mathcal{F}_a^T = -8C_F f_B \pi M_B^4 r_2 r_3 \int_0^1 dx_2 dx_3 \int_0^\infty b_2 b_3 db_2 db_3 \phi_2(x_2)\phi_3(x_3)\{x_2\alpha_s(t_e)h_e(\alpha_a, \beta_e, b_2, b_3) \times \exp[-S_{ef}(t_e)]S_t(x_3) + x_3\alpha_s(t_f)h_e(\alpha_a, \beta_f, b_3, b_2)\exp[-S_{ef}(t_f)]S_t(x_2)\}, \tag{A9}$$

$$\begin{aligned}\mathcal{M}_a^N = \frac{8}{3}C_F f_B \pi M_B^4 \int_0^1 dx_2 dx_3 \int_0^\infty b_1 b_2 db_1 db_2 \phi_2(x_2)\phi_3(x_3)\exp\left(-\frac{b_1^2\omega_B^2}{2}\right)\{[r_2^2(x_2-1) \\ + r_3^2(x_3-1)]\alpha_s(t_g)h_e(\beta_g, \alpha_a, b_1, b_2)\exp[-S_{gh}(t_g)] \\ - [r_2^2x_2 + r_3^2x_3 - 2r_2r_3r_b]\alpha_s(t_h)h_e(\beta_h, \alpha_a, b_1, b_2)\exp[-S_{gh}(t_h)]\},\end{aligned} \tag{A10}$$

$$\begin{aligned}\mathcal{M}_a^T = \frac{8}{3}C_F f_B \pi M_B^4 \int_0^1 dx_2 dx_3 \int_0^\infty b_1 b_2 db_1 db_2 \phi_2(x_2)\phi_3(x_3)\exp\left(-\frac{b_1^2\omega_B^2}{2}\right)\{[r_2^2(x_2-1) \\ - r_3^2(x_3-1)]\alpha_s(t_g)h_e(\beta_g, \alpha_a, b_1, b_2)\exp[-S_{gh}(t_g)] \\ - [r_2^2x_2 - r_3^2x_3]\alpha_s(t_h)h_e(\beta_h, \alpha_a, b_1, b_2)\exp[-S_{gh}(t_h)]\}.\end{aligned} \tag{A11}$$

For the CKM suppressed $B_c \to D_{(s)}^{*+}D^{*0}$ decays, the decay amplitudes for different polarizations are

$$\mathcal{F}^{L}_{e2} = -2\sqrt{\frac{2}{3}}C_F f_B f_3 \pi M_B^4 \int_0^1 dx_2 \int_0^\infty b_1 b_2 db_1 db_2 \phi_2(x_2) \exp\left(-\frac{b_1^2\omega_B^2}{2}\right)\{[-(r_2-2)r_b + 2r_2x_2 - x_2]\alpha_s(t_a)h_e(\alpha_e, \beta_a, b_1, b_2)S_t(x_2)\exp[-S_{ab}(t_a)] + r_2^2\alpha_s(t_b)h_e(\alpha_e, \beta_b, b_2, b_1)S_t(x_1)\exp[-S_{ab}(t_b)]\}, \tag{A12}$$

$$\mathcal{F}^{N}_{e2} = -2\sqrt{\frac{2}{3}}C_F f_B f_3 r_3 \pi M_B^4 \int_0^1 dx_2 \int_0^\infty b_1 b_2 db_1 db_2 \phi_2(x_2) \exp\left(-\frac{b_1^2\omega_B^2}{2}\right)\{[2 - r_b + r_2(4r_b - x_2 - 1)] \times \alpha_s(t_a)h_e(\alpha_e, \beta_a, b_1, b_2)S_t(x_2)\exp[-S_{ab}(t_a)] - r_2\alpha_s(t_b)h_e(\alpha_e, \beta_b, b_2, b_1)S_t(x_1)\exp[-S_{ab}(t_b)]\}, \tag{A13}$$

$$\mathcal{F}^{T}_{e2} = 2\sqrt{\frac{2}{3}}C_F f_B f_3 r_3 \pi M_B^4 \int_0^1 dx_2 \int_0^\infty b_1 b_2 db_1 db_2 \phi_2(x_2) \exp\left(-\frac{b_1^2\omega_B^2}{2}\right)\{[2 - r_b - r_2(1 - x_2)] \times \alpha_s(t_a)h_e(\alpha_e, \beta_a, b_1, b_2)S_t(x_2)\exp[-S_{ab}(t_a)] - r_2\alpha_s(t_b)h_e(\alpha_e, \beta_b, b_2, b_1)S_t(x_1)\exp[-S_{ab}(t_b)]\}, \tag{A14}$$

$$\mathcal{M}^{L}_{e2} = \frac{8}{3}C_F f_B \pi M_B^4 \int_0^1 dx_2 dx_3 \int_0^\infty b_2 b_3 db_2 db_3 \phi_2(x_2)\phi_3(x_3) \exp\left(-\frac{b_1^2\omega_B^2}{2}\right)\{[2 - x_1 - x_2 - x_3 - r_2(1 - x_2)] \times \alpha_s(t_c)h_e(\beta_c, \alpha_e, b_3, b_2)\exp[-S_{cd}(t_c)] - [x_3 - x_1 + r_2(1 - x_2)]\alpha_s(t_d)h_e(\beta_d, \alpha_e, b_3, b_2)\exp[-S_{cd}(t_d)]\}, \tag{A15}$$

$$\begin{aligned}\mathcal{M}^{N}_{e2} &= -\mathcal{M}^{T}_{e2}\\ &= \frac{8}{3}C_F f_B \pi M_B^4 \int_0^1 dx_2 dx_3 \int_0^\infty b_2 b_3 db_2 db_3 \phi_2(x_2)\phi_3(x_3) \exp\left(-\frac{b_1^2\omega_B^2}{2}\right)\{[r_3(x_1 - x_3)]\alpha_s(t_c)h_e(\beta_c, \alpha_e, b_3, b_2)\\ &\quad \times \exp[-S_{cd}(t_c)] + [2r_c - r_3(1 - x_1 - x_3)]\alpha_s(t_d)h_e(\beta_d, \alpha_e, b_3, b_2)\exp[-S_{cd}(t_d)]\}.\end{aligned} \tag{A16}$$

APPENDIX B: SCALES AND RELATED FUNCTIONS IN HARD KERNEL

We show here the functions h_e, coming from the Fourier transform of hard kernel,

$$h_e(\alpha, \beta, b_1, b_2) = h_1(\alpha, b_1) \times h_2(\beta, b_1, b_2),\ h_1(\alpha, b_1) = \begin{cases} K_0(\sqrt{\alpha}b_1), & \alpha > 0,\\ K_0(i\sqrt{-\alpha}b_1), & \alpha < 0,\end{cases}$$
$$\{h_2(\beta, b_1, b_2) = \begin{cases} \theta(b_1 - b_2)I_0(\sqrt{\beta}b_2)K_0(\sqrt{\beta}b_1) + (b_1 \leftrightarrow b_2), & \beta > 0,\\ \theta(b_1 - b_2)J_0(\sqrt{-\beta}b_2)K_0(i\sqrt{-\beta}b_1) + (b_1 \leftrightarrow b_2), & \beta < 0,\end{cases} \tag{B1}$$

where J_0 is the Bessel function and K_0, I_0 are modified Bessel functions with $K_0(ix) = \frac{\pi}{2}(-N_0(x) + iJ_0(x))$. The hard scale t is chosen as the maximum virtuality of the internal momentum transition in the hard amplitudes, including $1/b_i$ $(i = 1, 2, 3)$:

$$\begin{aligned} t_a &= \max\left(\sqrt{|\alpha_e|}, \sqrt{|\beta_a|}, 1/b_1, 1/b_2\right), & t_b &= \max\left(\sqrt{|\alpha_e|}, \sqrt{|\beta_b|}, 1/b_1, 1/b_2\right),\\ t_c &= \max\left(\sqrt{|\alpha_e|}, \sqrt{|\beta_c|}, 1/b_2, 1/b_3\right), & t_d &= \max\left(\sqrt{|\alpha_e|}, \sqrt{|\beta_d|}, 1/b_2, 1/b_3\right),\\ t_e &= \max\left(\sqrt{|\alpha_a|}, \sqrt{|\beta_e|}, 1/b_2, 1/b_3\right), & t_f &= \max\left(\sqrt{|\alpha_a|}, \sqrt{|\beta_f|}, 1/b_2, 1/b_3\right),\\ t_g &= \max\left(\sqrt{|\alpha_a|}, \sqrt{|\beta_g|}, 1/b_1, 1/b_2\right), & t_h &= \max\left(\sqrt{|\alpha_a|}, \sqrt{|\beta_h|}, 1/b_1, 1/b_2\right),\end{aligned} \tag{B2}$$

where

$$\begin{aligned}
&\alpha_e = (1-x_2)(x_1-r_2^2)(1-r_3^2)M_B^2, \qquad \alpha_a = -(1+(r_3^2-1)x_2)(1+(r_2^2-1)x_3)M_B^2,\\
&\beta_a = [r_b^2+(r_2^2-1)(x_2+r_3^2(1-x_2))]M_B^2, \qquad \beta_b = (1-r_3^2)(x_1-r_2^2)M_B^2,\\
&\beta_c = [r_c^2-(1-x_2(1-r_3^2))(1-x_1-x_3(1-r_2^2))]]M_B^2, \qquad \beta_d = (1-x_2)(1-r_3^2)[x_1-x_3-r_2^2(1-x_3)]M_B^2,\\
&\beta_e = -[1+(r_3^2-1)x_2]M_B^2, \qquad \beta_f = -[1+(r_2^2-1)x_3]M_B^2,\\
&\beta_g = [r_c^2+(1-x_2(1-r_3^2))(x_1+x_3-1-r_2^2x_3)]M_B^2, \qquad \beta_h = [r_b^2-x_2(r_3^2-1)(x_1-x_3(1-r_2^2))]M_B^2.
\end{aligned} \tag{B3}$$

The Sudakov factors used in the text are defined by

$$\begin{aligned}
S_{ab}(t) &= s\left(\frac{M_B}{\sqrt{2}}x_1, b_1\right) + s\left(\frac{M_B}{\sqrt{2}}x_2, b_2\right) + \frac{5}{3}\int_{1/b_1}^{t}\frac{d\mu}{\mu}\gamma_q(\mu) + 2\int_{1/b_2}^{t}\frac{d\mu}{\mu}\gamma_q(\mu),\\
S_{cd}(t) &= s\left(\frac{M_B}{\sqrt{2}}x_1, b_2\right) + s\left(\frac{M_B}{\sqrt{2}}x_2, b_2\right) + s\left(\frac{M_B}{\sqrt{2}}x_3, b_3\right) + \frac{11}{3}\int_{1/b_2}^{t}\frac{d\mu}{\mu}\gamma_q(\mu) + 2\int_{1/b_3}^{t}\frac{d\mu}{\mu}\gamma_q(\mu),\\
S_{ef}(t) &= s\left(\frac{M_B}{\sqrt{2}}x_2, b_2\right) + s\left(\frac{M_B}{\sqrt{2}}x_3, b_3\right) + 2\int_{1/b_2}^{t}\frac{d\mu}{\mu}\gamma_q(\mu) + 2\int_{1/b_3}^{t}\frac{d\mu}{\mu}\gamma_q(\mu),\\
S_{gh}(t) &= s\left(\frac{M_B}{\sqrt{2}}x_1, b_1\right) + s\left(\frac{M_B}{\sqrt{2}}x_2, b_2\right) + s\left(\frac{M_B}{\sqrt{2}}x_3, b_2\right), + \frac{5}{3}\int_{1/b_1}^{t}\frac{d\mu}{\mu}\gamma_q(\mu) + 4\int_{1/b_2}^{t}\frac{d\mu}{\mu}\gamma_q(\mu),
\end{aligned} \tag{B4}$$

where the functions $s(Q, b)$ are defined in Appendix A of Ref. [24]. $\gamma_q = -\alpha_s/\pi$ is the anomalous dimension of the quark.

APPENDIX C: MESON WAVE FUNCTIONS

In the nonrelativistic limit, the B_c meson wave function can be written as [33]

$$\Phi_{B_c}(x) = \frac{if_B}{4N_c}[(\not{P} + M_{B_c})\gamma_5\delta(x-r_c)]\exp\left(-\frac{b^2\omega_B^2}{2}\right), \tag{C1}$$

in which the last exponent term represents the k_T distribution. Here, we consider only the dominant Lorentz structure and neglect another contribution in our calculation [34].

In the heavy quark limit, the two-particle light-cone distribution amplitudes of $D_{(s)}/D_{(s)}^*$ meson are defined as [35]

$$\begin{aligned}
&\langle D_{(s)}(P_2)|q_\alpha(z)\bar{c}_\beta(0)|0\rangle\\
&\quad = \frac{i}{\sqrt{2N_c}}\int_0^1 dx e^{ixP_2\cdot z}[\gamma_5(\not{P}_2 + m_{D_{(s)}})\phi_{D_{(s)}}(x,b)]_{\alpha\beta},\\
&\langle D_{(s)}^*(P_2)|q_\alpha(z)\bar{c}_\beta(0)|0\rangle\\
&\quad = -\frac{1}{\sqrt{2N_c}}\int_0^1 dx e^{ixP_2\cdot z}[\not{\epsilon}_L(\not{P}_2 + m_{D_{(s)}^*})\\
&\qquad \times \phi_{D_{(s)}^*}^L(x,b) + \not{\epsilon}_L(\not{P}_2 + m_{D_{(s)}^*})\phi_{D_{(s)}^*}^T(x,b)]_{\alpha\beta},
\end{aligned} \tag{C2}$$

with the normalization conditions

$$\begin{aligned}
&\int_0^1 dx\phi_{D_{(s)}}(x,0) = \frac{f_{D_{(s)}}}{2\sqrt{2N_c}},\\
&\int_0^1 dx\phi_{D_{(s)}^*}^L(x,0) = \int_0^1 dx\phi_{D_{(s)}^*}^T(x,0) = \frac{f_{D_{(s)}^*}}{2\sqrt{2N_c}},
\end{aligned} \tag{C3}$$

where we have assumed $f_{D_{(s)}^*} = f_{D_{(s)}^*}^T$. Note that equations of motion do not relate $\phi_{D_{(s)}^*}^L$ and $\phi_{D_{(s)}^*}^T$. We use the following relations derived from heavy quark effective theory [36] to determine $f_{D_{(s)}^*}$:

$$f_{D_{(s)}^*} = \sqrt{\frac{m_{D_{(s)}}}{m_{D_{(s)}^*}}}f_{D_{(s)}}. \tag{C4}$$

The distribution amplitude $\phi_{D_{(s)}^{(*)}}^{(L,T)}$ is taken as [18]

$$\begin{aligned}
\phi_{D_{(s)}^{(*)}}^{(L,T)} &= \frac{3}{\sqrt{2N_c}}f_{D_{(s)}^{(*)}}x(1-x)[1 + a_{D_{(s)}^{(*)}}(1-2x)]\\
&\quad \times \exp\left(-\frac{b^2\omega_{D_{(s)}}^2}{2}\right).
\end{aligned} \tag{C5}$$

We use $a_D = 0.5 \pm 0.1$, $\omega_D = 0.1$ GeV for the D/D^* meson and $a_D = 0.4 \pm 0.1$, $\omega_{D_s} = 0.2$ GeV for the D_s/D_s^* meson, which are determined in Ref. [20] by fitting.

[1] N. Brambilla *et al.* (Quarkonium Working Group), arXiv:hep-ph/0412158.
[2] M. Masetti, Phys. Lett. B **286**, 160 (1992).
[3] R. Fleischer and D. Wyler, Phys. Rev. D **62**, 057503 (2000); R. Fleischer, Lect. Notes Phys. **647**, 42 (2004).
[4] V. V. Kiselev, J. Phys. G **30**, 1445 (2004); V. V. Kiselev, A. E. Kovalsky, and A. K. Likhoded, Nucl. Phys. **B585**, 353 (2000); V. V. Kiselev, arXiv:hep-ph/0211021.
[5] M. A. Ivanov, J. G. Körner, and O. N. Pakhomova, Phys. Lett. B **555**, 189 (2003).
[6] A. K. Giri, R. Mohanta, and M. P. Khanna, Phys. Rev. D **65**, 034016 (2002).
[7] M. A. Ivanov, J. G. Körner, and P. Santorelli, Phys. Rev. D **73**, 054024 (2006).
[8] J.-F. Liu and K.-T. Chao, Phys. Rev. D **56**, 4133 (1997).
[9] I. P. Gouz, V. V. Kiselev, A. K. Likhoded, V. I. Romanovsky, and O. P. Yushchenko, Phys. At. Nucl. **67**, 1559 (2004) [Yad. Fiz. **67**, 1581 (2004)].
[10] P. Colangelo and F. De Fazio, Phys. Rev. D **61**, 034012 (2000).
[11] A. Abd El-Hady, J. H. Munoz, and J. P. Vary, Phys. Rev. D **62**, 014019 (2000).
[12] C. H. Chang and Y. Q. Chen, Phys. Rev. D **49**, 3399 (1994).
[13] H.-Y. Cheng and C.-K. Chua, Phys. Rev. D **80**, 114008 (2009).
[14] H.-n. Li and H. L. Yu, Phys. Rev. Lett. **74**, 4388 (1995); H.-n. Li, Phys. Lett. B **348**, 597 (1995).
[15] Y. Y. Keum, H.-n. Li, and A. I. Sanda, Phys. Lett. B **504**, 6 (2001).
[16] C.-D. Lü, K. Ukai, and M.-Z. Yang, Phys. Rev. D **63**, 074009 (2001); C.-D. Lü and M. Z. Yang, Eur. Phys. J. C **23**, 275 (2002).
[17] C. W. Bauer, S. Fleming, D. Pirjol, and I. W. Stewart, Phys. Rev. D **63**, 114020 (2001); C. W. Bauer, D. Pirjol, and I. W. Stewart, Phys. Rev. Lett. **87**, 201806 (2001); Phys. Rev. D **65**, 054022 (2002).
[18] R.-H. Li, C.-D. Lü, and H. Zou, Phys. Rev. D **78**, 014018 (2008); H. Zou, R.-H. Li, X.-X. Wang, and C.-D. Lü, J. Phys. G **37**, 015002 (2010).
[19] Y. Li, C.-D. Lü, and C.-F. Qiao, Phys. Rev. D **73**, 094006 (2006); Y. Li and C.-D. Lü, J. Phys. G **29**, 2115 (2003).
[20] R.-H. Li, C.-D. Lü, A. I. Sanda, and X.-X. Wang, Phys. Rev. D **81**, 034006 (2010).
[21] Y. Li, C.-D. Lü, and Z.-J. Xiao, J. Phys. G **31**, 273 (2005).
[22] J. C. Collins and D. E. Soper, Nucl. Phys. **B193**, 381 (1981); J. Botts and G. Sterman, Nucl. Phys. **B325**, 62 (1989).
[23] B. Melic, B. Nizic, and K. Passek, Phys. Rev. D **60**, 074004 (1999).
[24] J.-F. Cheng, D.-S. Du, and C.-D. Lü, Eur. Phys. J. C **45**, 711 (2006).
[25] C.-D. Lü, Phys. Rev. D **68**, 097502 (2003); Y.-Y. Keum, T. Kurimoto, H.-n. Li, C.-D. Lü, and A. I. Sanda, Phys. Rev. D **69**, 094018 (2004).
[26] Particle Data Group, J. Phys. G **37**, 075021 (2010).
[27] W. Wang, Y. L. Shen, and C. D. Lü, Phys. Rev. D **79**, 054012 (2009).
[28] R. Dhir, N. Sharma, and R. C. Verma, J. Phys. G **35**, 085002 (2008); R. C. Verma and A. Sharma, Phys. Rev. D **65**, 114007 (2002); R. Dhir and R. C. Verma, Phys. Rev. D **79**, 034004 (2009).
[29] D.-S. Du and Z. Wang, Phys. Rev. D **39**, 1342 (1989).
[30] A. Ali, G. Kramer, and C.-D. Lü, Phys. Rev. D **58**, 094009 (1998).
[31] Y. Li and C.-D. Lü, Phys. Rev. D **73**, 014024 (2006).
[32] Z. Rui, Z.-T. Zou, and C.-D. Lü, arXiv:1112.1257.
[33] X. Liu, Z.-J. Xiao, and C.-D. Lü, Phys. Rev. D **81**, 014022 (2010).
[34] C.-D. Lü and M.-Z. Yang, Eur. Phys. J. C **28**, 515 (2003).
[35] T. Kurimoto, H. n. Li, and A. I. Sanda, Phys. Rev. D **67**, 054028 (2003).
[36] A. V. Manohar and M. B. Wise, Cambridge Monogr. Part. Phys., Nucl. Phys., Cosmol. **10**, 1 (2000).